Title
AN ANALYSIS OF SINGLE PION PHOTOPRODUCTION BETWEEN THRESHOLD AND 16 GeV

Author
Barbour, I.M.

Publication Date
1978-04-01

Submitted to Nuclear Physics B

LBL-7583
Preprint

c. 2

AN ANALYSIS OF SINGLE PION PHOTOPRODUCTION BETWEEN THRESHOLD AND 16 GeV

I. M. Barbour, R. L. Crawford, and
N. H. Parsons

April 1978

Prepared for the U. S. Department of Energy
under Contract W-7405-ENG-48

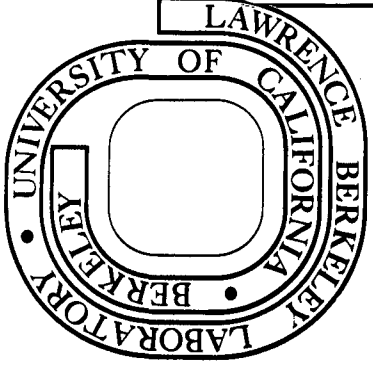

LBL-7583

C.2

DISCLAIMER

AN ANALYSIS OF SINGLE PION PHOTOPRODUCTION BETWEEN THRESHOLD AND 16 GeV[†]

I.M. Barbour, R.L. Crawford[*] and N.H. Parsons[**]

Department of Natural Philosophy,
The University, Glasgow G12 8QQ.

[†]This work was supported in part by the General Science and Basic Research Division of the United States Department of Energy.

[*]Work carried out during leave of absence at Lawrence Berkeley Laboratory, California.

[**]Now at Department of Theoretical Physics, 1 Keble Road, Oxford OX1 3NP.

Submitted to Nuclear Physics B

INTRODUCTION

This paper presents the results of the continuation of a previous analysis of single pion photoproduction[1]. As in that analysis our method consists of a multipole analysis at low energies, an amplitude analysis at high energies and a combination of both at intermediate energies. We use fixed-t dispersion relations as a constraint on our amplitudes and attempt to fit simultaneously to the data in the resonance region (C. of M. energy $W \lesssim 2$ GeV), the intermediate energy region ($2 \lesssim W \lesssim 2.5$ GeV) and the high energy region ($W \gtrsim 2.5$ GeV). This division of the data may appear to be somewhat arbitrary but in practice is a suitable way to combine parametrizations of the imaginary parts of the photoproduction amplitudes. This procedure, involving a simultaneous multipole and amplitude analysis, allows us to incorporate the general features of earlier fits to data in the resonance and the high energy region and to investigate their relative consistency in the intermediate energy region.

In sections 2, 3 and 4 we describe and discuss our results of two energy dependent analyses of the photoproduction data. We comment on the difficulties in extracting multipole amplitudes from the hybrid parametrization in the intermediate energy region. In section 5 we describe an energy independent method for treating this problem.

2. PARAMETRIZATION OF THE PHOTOPRODUCTION AMPLITUDES

The low energy parametrization for the imaginary parts of the photoproduction multipole amplitudes is identical to that used by Crawford[2] in an earlier low energy analysis.

In that fit the imaginary parts of resonance contributions were taken to have a Breit-Wigner structure aside from the P_{33} for which an Omnes-Muskhelishvilli form was used to impose the proper behaviour of the complex phase. Background contributions to the imaginary parts of the S-wave multipoles were included as broad Breit-Wigners.

The major difficulty inherent in such a parametrization arises from the divergence of the multipole expansion when it is used in the fixed-t dispersion relation and is consequently required for large negative unphysical values of $\cos\theta$, the C. of M. scattering angle[3]. In the previous fit we had to introduce a cut-off in the resonance region data set at $t = -1.5$ $(GeV/c)^2$ and in the high energy data set at $t = -.8$ $(GeV/c)^2$. In the fits presented below we have extended the high energy fit to $|t| \lesssim 1$ $(GeV/c)^2$ and suppress the high energy amplitudes in the fixed-t dispersion relation for $|t| > 1.2$ $(GeV/c)^2$ by a factor $e^{\lambda(1.2+t)}$ where the parameter λ is determined by the fit.

The difficulties due to the possible divergence of the multipole expansion would not have arisen had we used only an energy independent method to analyse the data. We would then have been able to cover the full physical momentum transfer region (but of course without the constraint of the fixed-t dispersion relations), and projection of the multipole amplitudes from our invariant amplitudes would then have followed a well defined procedure.

The high energy parametrization is essentially the same as that described by Barbour and Moorhouse[4]. Previous analyses[5] found that the fit to the π^o data was improved by the addition of an exotic exchange contribution to Im $A_3^{\pi^o}$ (s,t). Our earlier analysis found this exchange to be in the + isospin amplitude and we now constrain our amplitudes to satisfy (for $W \gtrsim 2.5$ GeV)

$$\text{Im } A_3^{0,-}(s,t) = 0$$

together with

$$\text{Im } A_1^{+,-,0}(s,t) = -t \text{ Im } A_2^{+,-,0}(s,t)$$

for ρ, ω and A_2 exchanges.

In the intermediate energy region we take the parametrization to be a combination of the above resonance and high energy parametrizations such that

$$\text{Im } A_i^{INT}(s,t) = \frac{1}{s_1-s_2} \text{ Im } \left\{(s-s_2)\, A_i^{RES}(s,t) + (s_1-s)\, A_i^{REG}(s,t)\right\} \qquad 2.1$$

for $\sqrt{s_1} = 2 \text{ GeV} < \sqrt{s} < 2.5 \text{ GeV} = \sqrt{s_2}$.

In this region, there is no longer a good understanding of the πN resonance structure and only the peripheral resonances have been definitely identified from πN partial wave analyses. Thus we are obliged to switch from the low energy to the high energy parametrizations and the hybrid form given above represents one of the simplest ways of achieving this. Im $A_i^{RES}(s,t)$ is parametrized using only the established $G_{17}(2190)$, $H_{19}(2220)$, $H_{3,11}(2420)$ resonances and the high energy tails of the lower energy resonances. If duality holds for the photoproduction amplitudes, Im $A_i^{REG}(s,t)$ should be in an average sense equivalent to

Im $A_i^{RES}(s,t)$. As a result, the parametrization of the $G_{17}(2190)$, $H_{19}(2220)$ and especially the $H_{3,11}(2420)$ does not truly describe the photoproduction of these resonances but is partly describing the local deviation of the Regge parametrization from the actual physical amplitudes. This implies that we cannot rely on the resonance parameters from the fit for W > 2 GeV but rather that the masses and widths of these resonances must come from an analysis of $A_i^{INT}(s,t)$. This we discuss below.

3. THE ENERGY DEPENDENT FITS

Tables I and II and Appendix 1 give the results of the two fits to the photoproduction data. The two fits were made independently to essentially the same data set (which is summarized in Appendix II). We attribute the differences in the results from the two fits mainly to random statistical effects and also to minor differences in the data sets used although we consider the latter to have a negligible effect.

The fitting procedures entailed calculating a χ^2 weighted in favour of the data in the energy region associated with the parameters being varied. It was not practical to minimize the χ^2 by varying all the parameters simultaneously but, as in our previous analysis, we frequently found that the fits to different regions were complementary since fitting in one region often improved the fit in other regions.

Information about the quality of the fits obtained is given in Table I and the corresponding resonance parameters are presented in Table IIa. Average values of our couplings are presented in Table IIb. Due to the complexity of the fitting program it was not practical to make

the usual error analyses for the couplings. However such errors are purely statistical in nature and are probably significantly less important than the systematic differences between various analyses such as the method of parametrization and the choice of data. To take account of this we have made subjective estimates of our statistical errors based on the variation of the parameters over a number of our fits and have combined them with estimates of possible systematic errors obtained by comparing the values obtained in a number of recent analyses[9,16]. The errors obtained cannot be considered as unique or even very objective but hopefully they give a useful and realistic assessment of the uncertainties in the couplings.

Although the χ^2 for the two fits differ, the resonance couplings below 2 GeV are essentially the same. However, the differences in the resonance couplings from the fits increase with the resonance energy, and this gives an indication of the uncertainty to be associated with values of the couplings. The neutron couplings seem to be particularly poorly determined, especially for the helicity 3/2 amplitudes and at W = 2 GeV the D_{35} and F_{17} have couplings which differ by a factor of two in the fits. As would be expected the peripheral resonances are, in general, the best determined with the prominent F_{37} obtaining close agreement between the fits.

In the intermediate region, both fits find the G_{17} with a mass of about 2.1 GeV and with similar couplings. At this energy the Breit-Wigner term is dominant (80% of total) and thus we consider that it is reasonable to use the Breit-Wigner couplings as the actual resonance couplings. On the other hand, the $H_{1,9}$ and $H_{3,11}$ do not show the same agreement between the fits. In the resonance parametrizations, both tend to lie at higher energies (about 2.3 GeV) than the $G_{1,7}$ and clearly interference between the Regge and resonance parametrizations is an important factor. Thus the analyses cannot at this stage give

their couplings and separate multipole analyses of the Regge plus resonance amplitudes must be made.

The two fits find the same leading Regge parameters for the imaginary parts of the photoproduction amplitudes above 2.5 GeV and marginally different values for the momentum dependence of the exotic exchange and amounts of natural parity daughter exchange.

In general, at all energies above the third resonance region, our fit to the π^o photoproduction data is not as good as that to the $\pi^\pm$ data. This could well be a reflection of the different dynamical mechanisms[6] governing single pion photoproduction at these energies. The real parts of the π^o amplitudes arise from delicate energy dependent interferences between each resonance and with the Regge contribution whereas for the $\pi^\pm$ amplitudes, the Born terms dominate in the forward direction and vary smoothly with energy. These amplitudes are hence less sensitive to a correct description of the energy dependence of the resonance and Regge contributions. This is an obvious limitation on any energy dependent analysis.

The χ^2 for the fits in the intermediate energy region is almost comparable to that for the fits below 2 GeV. However the data set for this region contains relatively few points.

Due to its preliminary nature we chose not to include the recent Daresbury measurements[7] of P, Σ and T for $\gamma P \to \pi^+ n$. However we obtain qualitative agreement with this data and we do not believe that the final results of this experiment will present us any difficulty. Similarly we were unable to use the preliminary measurements[8] of H at Daresbury. Figs. 1 and 2 show our predictions for G and H between E_γ = 0.6 and 1.6 GeV and gives a comparison with the Daresbury measurements of H. The rapid variation of G at $\theta = 120^o$ is a notable feature of our predictions.

4. DISCUSSION OF RESULTS

A comparison of the resonance couplings with those predicted by the quark model[9,10] reveals good qualitative agreement as shown in Table IIb.

In the $\{\overline{70},\ L = 1^-\}$ multiplet, however, disagreement is noted with the couplings predicted for the $S_{11}(1535)$, $S_{11}(1705)$ and the $A^n_{\frac{1}{2}}$ and $A^n_{3/2}$ of the D_{13} (1700).

However, by introducing some configuration mixing:-

$$S_{11}(1535) = \cos\theta\ \{(\bar{8},\ 2),\ J=\tfrac{1}{2}\} - \sin\theta\ \{(\bar{8},4),\ J=\tfrac{1}{2}\}$$

$$S_{11}(1705) = \cos\theta\ \{(\bar{8},\ 4),\ J=\tfrac{1}{2}\} + \sin\theta\ \{(\bar{8},2),\ J=\tfrac{1}{2}\}$$

with $\theta \simeq 30^o$, where $\{(\bar{8},\ 2S+1),\ J = \tfrac{1}{2}\}$ refers to the nucleon member of spin $\frac{1}{2}$ in the SU(3) octet of total quark spin S, we obtain reasonable agreement between our analysis and the quark model prediction for the S_{11} resonances. The disagreement of the quark model predictions for the $D_{13}(1700)$ can be explained when one takes into account of the large uncertainties in the numbers obtained by the analysis and the fact that, as we have already mentioned, these uncertainties are by no means unique statistical errors.

In the $\{\overline{56},\ L = 2^+\}$ multiplet good agreement is again revealed. Disagreements are evident, however, in the $A^{V3}_{\frac{1}{2}}$ amplitude of the $F_{35}(1890)$ the $A^{V3}_{3/2}$ amplitude of the $P_{33}(1690)$ and the $A^{V3}_{\frac{1}{2}}$ amplitude of the $P_{31}(1910)$. These quark model predictions may well be greatly improved by including a substantial quark spin-orbit term in the γN^* interaction as suggested by the Melosh transformation[11,12].

The quark model gives values of 30 and -50 for the $A^{V3}_{\frac{1}{2}}$ and $A^{V3}_{3/2}$ amplitudes, respectively, of the $P_{33}(1690)$, as compared with the values of 0 ± 30 obtained from our analysis.

Kubota and Ohta[13] apply relativistic "spin-orbit" corrections, which they obtain by applying the Foldy-Wouthuysen-Tani transformation on the relativistic Hamiltonian, to the non-relativistic quark model. They obtain much better agreement with the amplitudes of the F_{35}, P_{33} and P_{31}, as well as improved agreements with the $D_{13}(1520)$, $S_{11}(1535)$ and $F_{15}(1685)$. Substantial mixing of the S_{11}'s is still required, however.

An interesting observation in reference (12) is that when our amplitudes are analysed within the context of the Melosh transformation the relative sign of the P-wave and F-wave pionic decays of the $\{56, L = 2^+\}$ multiplet disagrees with that found in an analysis of $\pi N \to \pi\Delta$[14].

We would like to interpret this as evidence for the existence of a $\{\overline{70}, L = 2^+\}$ or $\{\overline{70}, L = 0^+\}$ multiplet, which mixes fairly strongly with the $\{\overline{56}, L = 2^+\}$. This ties in very well with our need for a resonance in the F_{17} wave at 1990 MeV. Such a resonance could only be assigned to a $\{\overline{70}, 2^+\}$ multiplet.

As usual the quark model predictions for the radial states are in disagreement with those of this analysis. These predictions, however, are extremely sensitive to the precise form used for the quark model wave-functions.

5. THE ENERGY INDEPENDENT FITS

As described above, the resonance parameters for the $H_{19}(2220)$ and $H_{311}(2420)$ are not determined by the above energy dependent fits. We therefore performed energy independent fits for $W < 2.5$ GeV to the

amplitudes obtained in the above fits ($|t| < 1.5$ (GeV/c)) together with differential cross-section data in the backward direction for $\pi^+ n$ and $\pi^o p$ photoproduction. This analysis must be considered exploratory in that the backward differential cross-section data places additional constraints only on $F_1 - F_2$. Our motivation at present is to study the stability of the multipole solutions obtained and hence to estimate how clearly they are determined.

The energy independent analysis is performed by treating the Born contributions exactly and fitting the remainder to the mulipole expansion cut off at $\ell \sim 9$. We find that the multipole amplitudes thus obtained are not sensitive to changes $|\Delta\ell| \leq 2$ for $W < 2.5$ GeV and that a good fit to the amplitudes obtained in the earlier fits and the backward data is maintained.

The results for the multipole amplitudes (without Born contributions) to which the G_{17}, H_{19} and H_{311} couple are shown in Figs. 3, 4 and 5. In general the two fits have qualitatively the same structures in each multipole but differ quantitatively in the energy dependence of the real background.

The resonance parameters for the H_{19} differ markedly between the two fits but Fig. 4 shows that the multipole amplitudes projected from the resonance and Regge contributions are remarkably similar. This illustrates our comments above concerning the need to consider the combined effects of the two parametrizations before extracting resonance couplings. One would conclude that the H_{19} has a mass between 2.1 and 2.15 GeV with a half width of about 0.15 to 0.2 GeV coupling predominantly to the electric multipole.

The H_{311} couples significantly to the M_{5+} multipole in both fits. In fit 2 the shape is distorted by a steadily increasing real background but the energy dependence of the imaginary parts obtained from both fits are very similar. The Becchi-Morpurgo[15] selection rule required that the H_{311} should only couple weakly to the electric multipole. As can be seen from Fig. 5 this selection rule is satisfied by Fit 1 but may or may not be satisfied by Fit 2. In both fits the imaginary part seems to be increasing steadily with energy and the difference between the two solutions appears to lie in the behaviour of their real parts.

We would consider the above analysis of the intermediate energy region encouraging, indicating that a more complete energy independent analysis linked to the amplitudes from the fixed-t dispersion relations could extract useful information about this energy region.

ACKNOWLEDGMENTS

The authors wish to thank the Lawrence Berkeley Laboratory and Daresbury Laboratory for computing facilities. One of us (RLC) wishes to express his gratitude to the Particle Data Group at Lawrence Berkeley Laboratory for their hsopitality during a visit in 1976-77 when part of the above analysis was performed and to thank R. Kelly and A. Rittenberg for assistance and discussions.

APPENDIX I

We list here the imaginary parts of the photoproduction isoscalar (0) and isovector (+,-) invariant amplitudes valid for W > 2.5 GeV as found in fit I. The parameters obtained in fit II are given in brackets when they differ significantly from those of fit I. These amplitudes also contribute to the imaginary parts of the photoproduction amplitudes for 2.0 GeV < W < 2.5 GeV when combined as in equation 2.1 with the Breit-Wigner contributions summarized in Table IIa

The amplitudes are normalized as in reference (17) and 1 GeV is taken as the unit of energy.

$$\text{Im } A_1^o = \left[0.39e^{-2.8t} \overset{(0.24)}{-0.26} \left(\frac{s_o}{s}\right) e^{-3.0t}\right] J_2 \left(\frac{s}{s_o}\right)^{\alpha_\rho - 1}$$

$$\text{Im } A_1^- = \left[0.25e^{-2.9t} \overset{(7.42)}{+ 6.79} \left(\frac{s_o}{s}\right) e^{5.5t}\right] J_2 \left(\frac{s}{s_o}\right)^{\alpha_{A_2} - 1}$$

$$\text{Im } A_1^+ = \left\{0.48e^{\overset{(0.68)}{-0.41t}} J_4 + \left[-0.93e^{\overset{(+1.8)}{+2.1t}} \overset{(3.05)}{+ 3.73} \left(\frac{s_o}{s}\right) e^{1.4t}\right] J_2\right\} \left(\frac{s}{s_o}\right)^{\alpha_\omega - 1}$$

$$\text{Im } t\, A_2^o = -\text{Im } A_1^o + 0.29e^{\overset{(-0.54)}{-0.87t}} J_2 \left(\frac{s}{s_o}\right)^{\alpha_B - 1}$$

$$\text{Im } t\, A_2^- = -\text{Im } A_1^-$$

$$\text{Im } t\, A_2^+ = -\text{Im } A_1^+$$

$$\text{Im } A_3^o = 0$$

$$\text{Im } A_3^- = 0$$

$$\text{Im } \sqrt{-t}\, A_3^+ = -32.6e^{\overset{(+2.0)}{+0.96t}} J_1 \left(\frac{s}{s_o}\right)^{\alpha_v - 1}$$

$$\text{Im } \sqrt{-t}\, A_4^o = 0.33e^{\overset{(15.0)}{12.0t}} J_1 \left(\frac{s}{s_o}\right)^{\alpha_\rho - 1}$$

$$\text{Im } \sqrt{-t}\, A_4^- = 0.19e^{\overset{(-1.9)}{-1.4t}} J_1 \left(\frac{s}{s_o}\right)^{\alpha_{A_2} - 1}$$

$$\text{Im}\sqrt{-t}\,A_4^+ = \left\{2.51e^{-1.3t}\,J_1 - 0.11e^{+0.51t}\,J_3\right\}\left(\frac{s}{s_o}\right)^{\alpha_\omega - 1}$$

with $s_o = 2\ \text{GeV}^2$.

The Bessel functions J_n are functions of $R\sqrt{-t}$ with $R = 1.05F$. In both fits the cut-off parameter λ was found to be small $\lambda = 0.2\ (\text{GeV/c})^{-1}$ for fit I and $-0.4\ (\text{GeV/c})^2$ for fit II. The trajectories for the Regge exchanges included were found to be

$\alpha_\rho = 0.48 + 1.00t$ $\qquad$ $\alpha_B = 0.025 + 1.05t$

$\alpha_{A_2} = 0.43 + 0.99t$ $\qquad$ $\alpha_v = -3.0 + 1.5t$

$\alpha_\omega = 0.34 + 1.05t$

APPENDIX II

SOURCES OF EXPERIMENTAL DATA USED IN THE ANALYSIS

$\gamma p \rightarrow \pi^+ n$ differential cross sections

M.I. Adamovich et al. Sov. Jour. Nucl. Phys. 7 (1968) 360; JETP 26 (1968) 344.

Yu. M. Aleksandrov et al. JEPT 22 (1966) 39.

Yu. M. Aleksandrov et al. Sov. Jour. Nucl. Phys. 12 (1971) 416.

R.A. Alvarez Phys. Rev. 142 (1966) 957.

R.A. Alvarez et al. Phys. Rev. D1 (1970) 1946.

Z. Bar-Yam et al. Phys. Rev. Letts. 19 (1967) 40.

Z. Bar Yam et al. Phys. Rev. Letts. 25 (1970) 1053.

C. Betourne et al. Phys. Rev. 172 (1968) 1343.

M. Beneventano et al. Nuovo Cimento 54 (1968) 468.

B. Bouquet et al. Phys. Rev. Letts. 27 (1971) 1244.

A.M. Boyarski et al. Phys. Rev. Letts. 20 (1967) 300.

A.M. Boyarski et al. Contribution to Vienna Conference 1969.

H. Burfeindt et al. Phys. Letts. 33B (1970) 509.

G. Buschhorn et al. Phys. Rev. Letts. 17 (1966) 1027.

G. Buschhorn et al. Phys. Rev. Letts. 18 (1967) 571.

G. Buschhorn et al. Phys. Letts. 25B (1967) 622.

S.D. Ecklund and R.L. Walker Phys. Rev. 159 (1967) 1195.

S.D. Ecklund Caltech thesis 1966.

K. Ekstrand et al. Phys. Rev. D6 (1972) 1.

G. Fischer et al. BONN-PIB-1-100 (1970).

G. Fischer et al. Nucl. Phys. B16 (1970) 119; Z. Phys. 253 (1972) 38.

T. Fujii et al. Phys. Rev. Letts. 26 (1971) 1672.

P. Heide et al. Phys. Rev. Letts. 21 (1968) 248.

P.M. Joseph et al. Phys. Rev. Letts. 19 (1967) 1206.

J.R. Kilner Caltech thesis (1963).

H.A. Thiessen Phys. Rev. 155 (1967) 1488; Caltech thesis (1966).

$\gamma p \rightarrow \pi^+ n$ Polarized photon asymmetry (Σ)

L.O. Abrahamian et al. Phys. Letts. B48 (1974) 463.

L.O. Abrahamian et al. EFI-136, Yerevan preprint (1975).

J. Alspector et al. Phys. Rev. Letts. 28 (1972) 1403.

V.B. Ganenko et al. Sov. Jour. Nucl. Phys. 23 (1970) 100.

C. Geweniger et al. Phys. Letts. 29B (1969) 41.

M. Grilli et al. Phys. Letts. 19 (1965) 157; Phys. Letts. 23 (1966) 394.

G. Knies et al. Phys. Rev. D10 (1974) 2778.

V.M. Kuznetsov Sov. Jour. Nucl. Phys. 13 (1971) 603;
JEPT Letts. 10 (1969) 273.

F.F. Liu, D.J. Drickey and R.F. Mozley Phys. Rev. B136 (1964) 1183.

D.J. Sherden et al. Contribution to Bonn Conf. (1973).

R.C. Smith and R.F. Mozley Phys. Rev. 130 (1963) 2429.

V.N. Zabaev et al. Sov. Jour. Nucl. Phys. 21 (1975) 551.

R.W. Zdarko and E.B. Dally Nuovo Cimento 10A (1972) 10.

$\gamma p \rightarrow \pi^+ n$ Recoil nucleon polarization (P)

K.H. Althoff et al. Phys. Letts. 26B (1968) 640.

M. Hahn, H. Heinrichs and W. Wallraff Bonn preprint PIB-1-143 (1971).

W. Wallraff Bonn thesis PIB-1-162 (1972).

$\gamma p \rightarrow \pi^+ n$ Polarized Target Asymmetry (T)

K.H. Althoff et al. Nucl. Phys. B53 (1973) 9.

K.H. Althoff et al. Phys. Letts. 59B (1975) 93.

K.H. Althoff et al. Phys. Letts. 63B (1976) 107.

S. Arai et al. Phys. Letts 40B (1972) 426, Nucl. Phys. B48 (1972) 379.

P. Feller et al. Nucl. Phys. B102 (1976) 207.

C.C. Morehouse et al. Phys. Rev. Letts. 25 (1970) 835.

$\gamma p \rightarrow \pi^o p$ differential cross section

R. Alvarez et al. Phys. Rev. Letts. 12 (1964) 707.

R.L. Anderson et al. Phys. Rev. D4 (1971) 1937.

C. Bacci et al. Phys. Rev. 159 (1967) 1124.

J.S. Barton et al. Nucl. Phys. B84 (1975) 449.

H. Becks et al. Nucl. Phys. B60 (1973) 267.

P.S.L. Booth et al. Nuovo Cimento 13A (1973) 235.

P.S.L. Booth et al. Nucl. Phys. B84 (1974) 437.

M. Braunschweig et al. Phys. Letts. 26B (1968) 405.

M. Braunschweig et al. Nucl. Phys. B20 (1970) 191.

W. Brefeld et al. Nucl. Phys. B100 (1975) 93.

G. Buschhorn et al. Phys. Rev. Letts. 20 (1968) 230.

G.L. Cassidy et al. Phys. Rev. Letts. 21 (1968) 933.

M. Croisseaux et al. Phys. Rev. 164 (1967) 1623.

H. de Staebler et al. Phys. Rev. 140 (1965) B336.

B. Delcourt et al. Phys. Letts. 29B (1969) 70.

P. Feller et al. Phys. Letts. 49B (1974) 197.

H. Genzel et al. Zeit. Phys. 268 (1974) 43.

B.B. Govorkov et al. Sov. Jour. Nucl. Phys. 4 (1967) 265.

G.L. Hatch Caltech. thesis (1967).

Y. Hemmi et al. Nucl. Phys. B55 (1973) 333.

V.L. Highland Phys. Rev. 132 (1963) 1293.

A.P. Hufton Liverpool thesis (1973).

B. Lohr Bonn PIB-1-98.

R. Morand et al. Phys. Rev. 180 (1969) 1299.

R.M. Talman et al. Phys. Rev. Letts. 9 (1962) 177.

F.B. Wolverton Caltech thesis (1968).

N. Yoshioka et al. Tokyo preprint INS-281 (1977).

We did not include the Lund data (P. Dougan et al. Zeit Phys. A274 (1975) 73 and Zeit Phys. 276 (1976) 155) due to a mis-match of the normalisation of the data with other data for E_γ below 500 MeV.

$\gamma p \rightarrow \pi^o p$ Polarized Photon Asymmetry (Σ)

L.O. Abrahamian et al. Phys. Letts 48B (1974) 463.

L.O. Abrahamian et al. Yerevan preprint EFI-136 (1975).

R.L. Anderson et al. Phys. Rev. D4 (1971) 1937.

J. Alspector et al. Phys. Rev. Letts 28 (1972) 1403.

G. Barbiellini et al. Phys. Rev. 184 (1969) 1402.

D. Bellenger et al. Phys. Rev. Letts. 23 (1969) 540.

G. Bologna et al. Frascati preprint LNF-70/39 (1970).

P.J. Bussey et al. Nucl. Phys. B104 (1976) 253.

D.R. Drickey & R.F. Mozley Phys. Rev. 136 (1964) B543.

V.B. Ganenko et al. Sov. Jour. Nucl. Phys. 20 (1974) 356.

V.B. Ganenko et al. Sov. Jour. Nucl. Phys. 23 (1976) 310.

G. Knies et al. Phys. Rev. D10 (1974) 2778.

R.W. Zdarko & E.B. Dally Nuovo Cimento 10A (1972) 10.

$\gamma p \rightarrow \pi^o p$ Recoil Nucleon Polarisation (P)

K.H. Althoff et al. Zeit Phys. 194 (1966) 135.

K.H. Althoff et al. Zeit Phys. 194 (1966) 144.

K.H. Althoff et al. Phys. Letts. 26B (1968) 677.

L. Bertanza et al. Nuovo Cimento 24 (1962) 734.

L. Bertanza et al. Nuovo Cimento 19 (1961) 953.

E.D. Bloom et al. Phys. Rev. Letts. 19 (1967) 671.

P. Blüm et al. Phys. Letts. 32B (1970) 137.

P. Blüm et al. Zeit Phys. A277 (1976) 311.

P. Blüm et al. Zeit Phys. A278 (1976) 275.

M. Deutsch et al. Phys. Rev. Letts. 29 (1972) 1752.

A.I. Derebchinskii et al. JETP 66 (1974) 68.

N.V. Goncharov et al. JETP 64 (1973) 401.

S. Hayakawa et al. Jour. Phys. Soc. Japan 25 (1968) 307.

N. Tanaka et al. Phys. Rev. D8 (1973) 1.

D. Trines Bonn PIB-1-160 (1972).

$\gamma p \rightarrow \pi^{o} p$ Polarized Target Asymmetry (T)

H. Beinlein et al. Phys. Letts. 46B (1973) 131.

P.S.L. Booth et al. Phys. Letts. 38B (1972) 339.

P.S.L. Booth et al. Daresbury report DL-P-270 (1976).

P. Feller et al. Nucl. Phys. B110 (1976) 397.

$\gamma n \rightarrow \pi^{-} p$ Differential Cross-section and π^{-}/π^{+} Ratio (R)

Z. Bar-Yam et al. Phys. Rev. Letts. 19 (1967) 40.

P. Benz et al. Nucl. Phys. B65 (1973) 158.

M. Beneventano et al. Nuovo Cimento 19A (1974) 529.

A.M. Boyarski Phys. Rev. Letts. 21 (1968) 1767.

T. Fujii et al. Phys. Rev. Letts. 26 (1971) 244.

T. Fujii et al. Nucl. Phys. B120 (1977) 395.

P. Hiede et al. Phys. Rev. Letts. 21 (1968) 248.

A. Ito et al. Phys. Rev. Letts. 24 (1970) 687.

G. Neugebauer et al. Phys. Rev. 119 (196) 1726.

P.E. Scheffler and P.L. Walden Nucl. Phys. B75 (1974) 125.

$\gamma n \rightarrow \pi^- p$ Polarized Photon Asymmetry (Σ)

J. Alspector et al. Phys. Rev. Letts. 28 (1972) 1403.

Z. Bar Yam et al. Phys. Rev. Letts. 24 (1970) 1078.

G. Knies et al. Phys. Rev. D10 (1974) 2778.

K. Kondo et al. Phys. Rev. Letts. 21 (1968) 1288.

F.F. Lui, D.J. Drickey and R.F. Mozley Phys. Rev. B136 (1964) 1183.

D.J. Sherden et al. Phys. Rev. Letts. 30 (1973) 1230.

No data for the reaction $\gamma n \rightarrow \pi^- p$ (or $\gamma n \rightarrow \pi^o n$) were used for photon laboratory energies below 500 MeV to allow the $P_{33}(1232)$ to be studied solely as a Δ^+ state. However a good prediction of the data in this region was obtained.

$\gamma n \rightarrow \pi^o n$ and $\gamma p \rightarrow \pi^o p$ - ratio of differential cross-sections

W. Braunschweig et al. Nucl. Phys. B51 (1973) 157.

A.M. Osborne et al. Phys. Rev. Letts. 29 (1972) 1621.

REFERENCES

1. I.M. Barbour & R.L. Crawford Nucl. Phys. B111 (1976) 358.

2. R.L. Crawford Nucl. Phys. B97 (1975) 125.

3. R.C.E. Devenish, W.J. Leigh, D.H. Lyth, W.A. Rankin
   Nuovo Cimento 1A (1971) 155.
   R.C.E. Devenish, D.H. Lyth & W.A. Rankin Daresbury report
   DNPL/P 109 (1972).

4. I.M. Barbour & R.G. Moorhouse Nucl. Phys. B69 (1974) 637.

5. I.S. Barker, A. Donnachie & J.K. Storrow Nucl. Phys. B79 (1974) 431.

6. I.M. Barbour, W. Malone & R.G. Moorhouse Phys. Rev. D4 (1971) 1521.

7. P.J. Bussey, C. Raine, J.G. Rutherglen, P.S.L. Booth, L.J. Carroll, G.R. Court, P. Daniel, A. Edwards, R. Gamet, C.J. Hardwick, P.J. Hayman, J.R. Holt, W.H. Range, F.H. Combley, W. Galbraith, V.H. Rajaratnam and C. Sutton, Contribution no. 125 to the International Symposium on Lepton & Photon Interactions at High Energies, Stanford, August 1975; W.H. Range, Contribution to the Topical Conference on Baryon Resonances, Oxford, 1976.

8. P.J. Bussey, J.G. Rutherglen, P.S.L. Booth, L.J. Carroll, G.R. Court, P.R. Daniel, A.W. Edwards, R. Gamet, P.J. Hayman, J.R. Holt, J.N. Jackson, W.H. Range, C. Wooff, F.H. Combley, W. Galbraith, A. Phillips & V.H. Rajaratnam Contribution to Oxford Conference 1976.

9. R.G. Moorhouse & H. Oberlack Phys. Letts. 43B (1973) 44;
   R.G. Moorhouse, H. Oberlack & A.H. Rosenfeld Phys. Rev. D9 (1974) 1;
   G. Knies, R.G. Moorhouse & H. Oberlack LBL 2410 (1974).

10. R.P. Feynman, M. Kislinger & F. Ravndal Phys. Rev. D3 (1971) 2706.

11. A.J.G. Hey, P.J. Litchfield & R.J. Cashmore Nucl. Phys. B98 (1975) 237.

12. J. Babcock, J.L. Rosner, R.J. Cashmore & A.J.G. Hey
    Nucl. Phys. B126 (1977) 87.

13. T. Kubota & K. Ohta Phys. Letts. 65B (1976) 374.

14. A.J.G. Hey & J. Weyers Phys. Letts. 48B (1974) 69;
    E. Gilman & I. Karliner Phys. Rev. D10 (1974) 2194;
    A.J.G. Hey, P.J. Litchfield & R.J. Cashmore Nucl. Phys. B95
    (1975) 516.

15. C. Becchi & G. Morpurgo Phys. Letts. 17, (1965) 352.

16. R.C.E. Devenish, D.H. Lyth & W.A. Rankin Phys. Letts. 52B (1974) 227.
    W.J. Metcalf & R.L. Walker Nucl. Phys. B76 (1974) 253.
    P. Feller, M. Fukushima, N. Horikawa, R. Kajikawa, K. Mori, T. Nakanishi, T. Okshima, C.O. Pak, M. Saito, S. Suzuji, Y. Tarui & Y. Yamaki
    Nucl. Phys. B104 (1976) 219.

17. F.A. Berends, A. Donnachie & D.L. Weaver Nucl. Phys. B4 (1967) 1.

TABLE CAPTIONS

Table I — The χ^2 for the two fits to the data in the low, intermediate and high energy regions.

Table IIa — The couplings, masses and widths for the two fits. All the masses and widths except for the $P_{33}(1690)$ were varied during the fitting.

Table IIb — The average couplings from the two fits compared with the predictions of the quark model. The method of obtaining the errors and their significance are discussed in the text. The asterisks indicate quark model predictions which are free from strong cancellations and hence those whose signs can be considered to be well determined.

TABLE I

Type of data	Fit	Threshold to W=2.0GeV		2.0<W<2.5 GeV		W=2.5GeV to 5.6GeV	
		No. of data	χ^2/N	No. of data	χ^2/N	No. of data	χ^2/N
$\gamma p \to \pi^+ n$ differential cross section	1	2140	1.59	46	1.87	83	1.76
	2	2182	1.53	46	1.60	83	1.87
$\gamma p \to \pi^+ n$ recoil nucleon polarisation	1	26	2.88	-	-	-	-
	2	26	3.22	-	-	-	-
$\gamma p \to \pi^+ n$ polarised photon asymmetry	1	207	1.83	14	1.18	22	1.23
	2	261	1.51	9	0.67	22	1.18
$\gamma p \to \pi^+ n$ polarised target asymmetry	1	61	2.48	7	4.90	10	0.70
	2	61	2.06	7	4.30	10	0.78
$\gamma p \to \pi^o p$ differential cross section	1	2194	3.06	61	8.35	97	3.31
	2	2033	2.71	61	4.80	97	3.14
$\gamma p \to \pi^o p$ recoil nucleon polarisation	1	197	3.03	1	0.60	12	1.27
	2	207	2.90	1	0.11	12	1.38
$\gamma p \to \pi^o p$ polarised photon asymmetry	1	252	5.18	101	2.93	25	1.07
	2	263	4.24	123	1.57	25	1.10
$\gamma p \to \pi^o p$ polarised target asymmetry	1	149	1.69	18	1.36	35	2.60
	2	141	1.68	18	0.95	35	2.85
$\gamma n \to \pi^- p$ differential cross section	1	491	1.77	8	2.89	3	1.19
	2	491	1.57	9	2.27	3	1.56
$\gamma n \to \pi^- p$ polarised photon asymmetry	1	113	2.49	9	3.67	14	5.31
	2	113	2.21	8	1.42	14	5.08
$\gamma n \to \pi^- p / \gamma p \to \pi^+ n$ ratio of differential cross sections	1	101	2.24	1	6.74	56	1.15
	2	101	2.21	1	10.66	56	1.15
$\gamma n \to \pi^o n / \gamma p \to \pi^o p$ ratio of differential cross sections	1	0	-	0	-	20	0.76
	2	0	-	0	-	20	0.75
Totals	1	5931	2.40	266	3.87	377	2.10
	2	5879	2.15	283	2.32	377	2.10

TABLE IIa

Resonance	Fit	Mass (MeV)	Width (MeV)	Couplings $(GeV)^{-\frac{1}{2}} \times 10^3$ $A^p_{1/2}$	$A^p_{3/2}$	$A^n_{1/2}$	$A^n_{3/2}$
$P_{11}(1470)$	1	1415	331	-74	-	58	-
	2	1419	331	-75		60	
$D_{13}(1520)$	1	1504	137	-14	157	-56	-138
	2	1502	133	-18	157	-54	-144
$S_{11}(1535)$	1	1510	133	75	-	-111	-
	2	1512	130	88		-112	
$D_{15}(1670)$	1	1682	195	18	12	-66	-73
	2	1677	189	25	7	-66	-72
$F_{15}(1685)$	1	1679	119	-4	138	37	-36
	2	1681	118	-5	138	36	-39
$S_{11}(1700)$	1	1689	197	50	-	-38	-
	2	1698	188	45		-52	
$D_{13}(1705)$	1	1726	100	-27	-8	49	15
	2	1712	151	-38	-19	50	54
$P_{11}(1780)$	1	1735	128	-2	-	-34	-
	2	1706	205	3		-21	
$P_{13}(1810)$	1	1807	271	110	-57	13	42
	2	1810	299	111	-68	0	60
$F_{17}(1990)$	1	1990	210	46	13	-93	-43
	2	2008	221	34	-6	-45	-100
$G_{17}(2190)$	1	2135	201	-41	180	-83	-5
	2	2098	238	-18	179	-87	19
$P_{33}(1232)$	1	1231.1	111.3	-141	-269	-	-
	2	1231.2	110.7	-143	-272		
$S_{31}(1650)$	1	1666	201	40	-	-	-
	2	1657	159	28			
$D_{33}(1670)$	1	1629	217	136	98	-	-
	2	1628	214	123	98		
$P_{33}(1690)$	1	-	-	-	-	-	-
	2	1690	225	0	0	-	-
$F_{35}(1890)$	1	1899	132	35	-59	-	-
	2	1844	186	31	-51		
$P_{31}(1910)$	1	1936	208	-37	-	-	-
	2	1861	252	-32			
$F_{37}(1950)$	1	1911	175	-58	-79	-	-
	2	1913	220	-58	-71		
$D_{35}(2000)$	1	2024	489	-81	10	-	-
	2	2024	434	-43	27		
$H_{19}(2220)$	1	2184	303	1	29	-13	-27
	2	2345	284	-43	110	67	-19
$H_{3,11}(2420)$	1	2394	327	-21	-33	-	-
	2	2303	324	0	-70		

Table IIb

Resonance	Mass (MeV)	Width (MeV)	Couplings $(GeV)^{-\frac{1}{2}} \times 10^3$							
			$A^p_{\frac{1}{2}}$	$A^p_{\frac{1}{2}}$(QM)	$A^p_{3/2}$	$A^p_{3/2}$(QM)	$A^n_{\frac{1}{2}}$	$A^n_{\frac{1}{2}}$(QM)	$A^n_{3/2}$	$A^n_{3/2}$(QM)
$P_{11}(1470)$	1417	331	-75±15	27	-	-	59±16	-18	-	-
$D_{13}(1520)$	1503	135	-16± 8	-34	157± 7	109*	-55±14	-31	-141 15	-109*
$S_{11}(1535)$	1511	132	82±19	156	-	-	-112±34	-108	-	-
$D_{15}(1670)$	1680	192	22±10	0*	15± 6	0*	-66±20	-38*	-73±14	-53*
$F_{15}(1685)$	1680	119	-5±15	-10	138±21	60*	37±10	30*	-38±18	0*
$S_{11}(1700)$	1694	193	48±17	0	-	-	-45±24	30	-	-
$D_{13}(1705)$	1719	126	-33±21	0*	-14±25	0*	50±42	-10*	35±30	-40*
$P_{11}(1780)$	1721	167	1±39	-40	-	-	-28±45	10	-	
$P_{13}(1810)$	1809	285	111±47	100	-63±32	-30	7±20	-30	51±51	0*
$F_{17}(1990)$	1999	216	40		4		-69		-72	
$P_{33}(1232)$	1231.2	111	-142± 7	-108*	-271±10	-187*	-	-	-	-
$S_{31}(1650)$	1662	180	34±28	47	-	-	-	-	-	-
$D_{33}(1670)$	1629	216	130±37	88	98±36	84*	-	-	-	-
$P_{33}(1690)$	1690	225	0±30	23	0±45	39	-	-	-	-
$F_{35}(1890)$	1892	159	33±18	-20*	-55±19	-90*	-	-	-	-
$P_{31}(1910)$	1899	230	-35±21	30	-	-	-	-	-	-
$F_{37}(1950)$	1912	198	-58±13	-50*	-75±20	-70*	-	-	-	-
$D_{35}(2000)$	2024	462	-62±64		19±54		-	-	-	-
$G_{17}(2190)$	2117	220	-30		180		-85		7	

FIGURE CAPTIONS

Fig. 1 Predictions for the asymmetry parameter G from fit 2. The predictions of fit 1 are essentially identical.

Fig. 2 Comparison of the predictions from fit 2 for the asymmetry parameter H with the Daresbury measurements. The predictions of fit 1 are essentially the same.

Fig. 3 Argand diagrams for the G_{17} multipoles in the intermediate region. The Born term contributions to the real parts are not included. Fit 1 is given by the dashed line and fit 2 by the solid line. The units correspond to $\hbar$, c and the pion mass set equal to one.

Fig. 4 Argand diagrams for the H_{19} multipoles. The same comments as in Fig. 3 apply.

Fig. 5 Argand diagrams for the $H_{3,11}$ multipoles. The same comments as in Fig. 3 apply.

Fig. 1

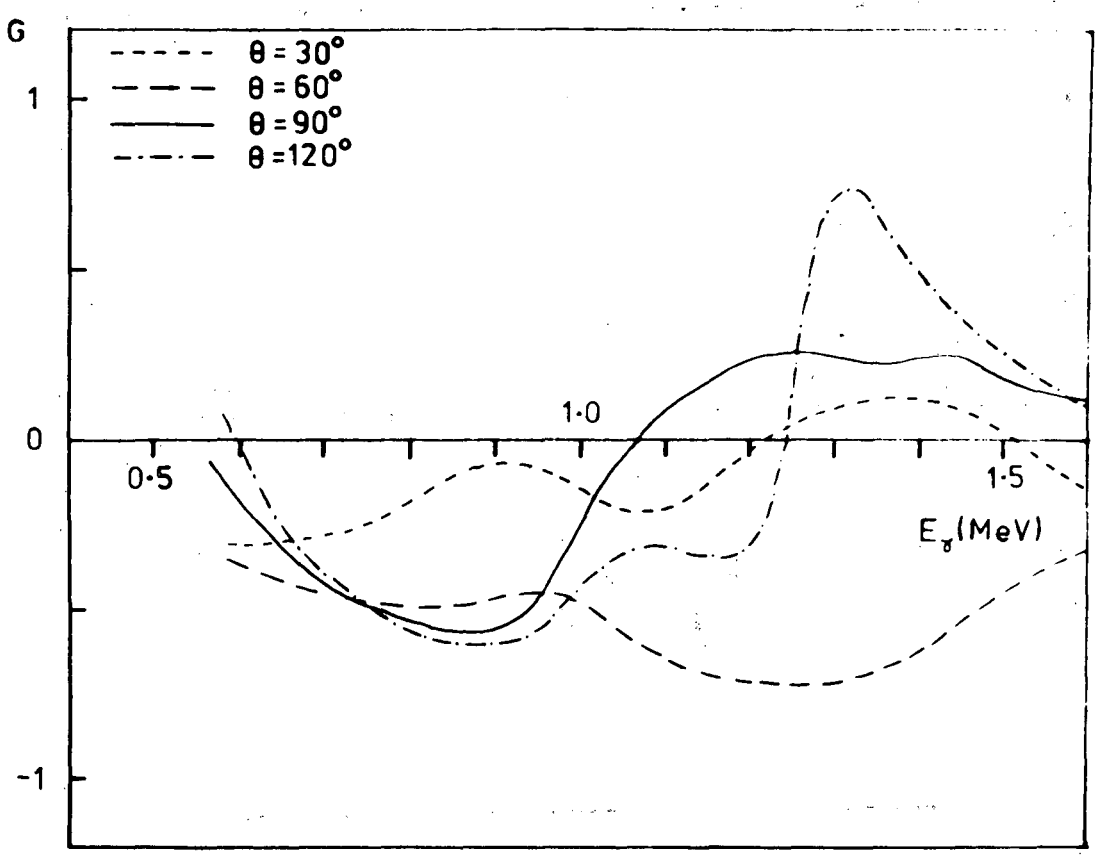

Fig. 2a

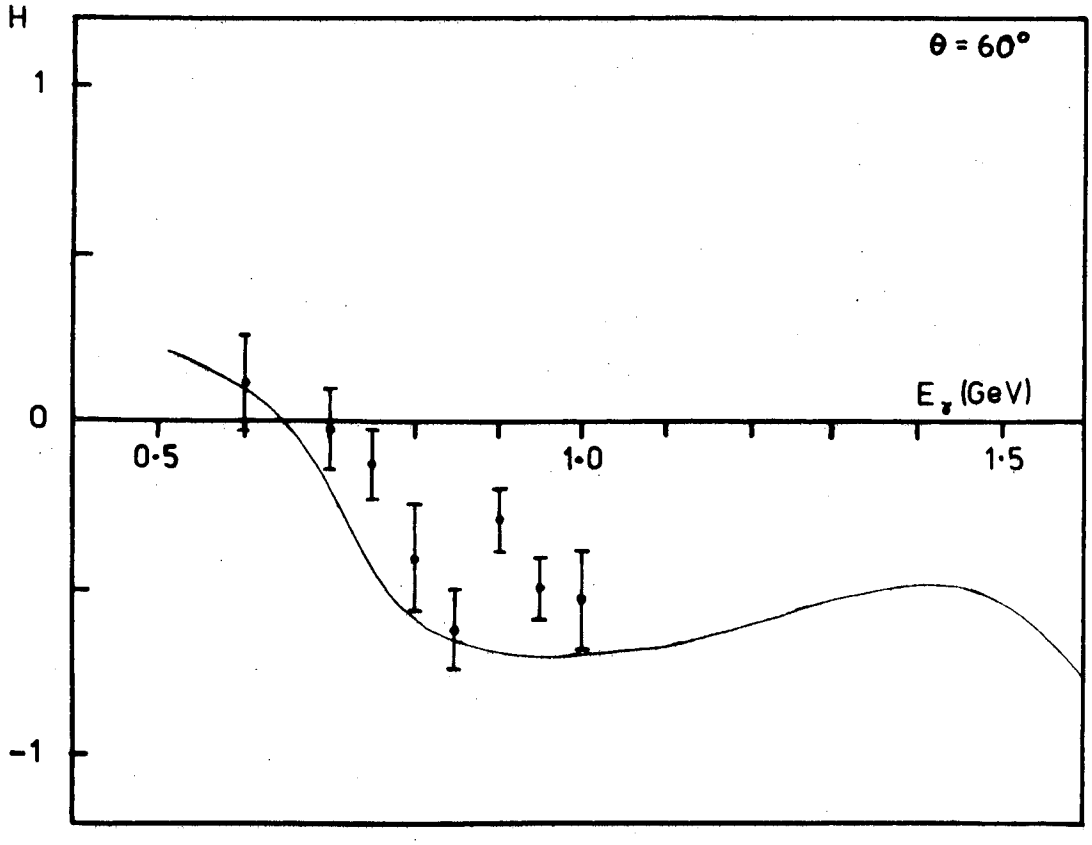

Fig. 2b

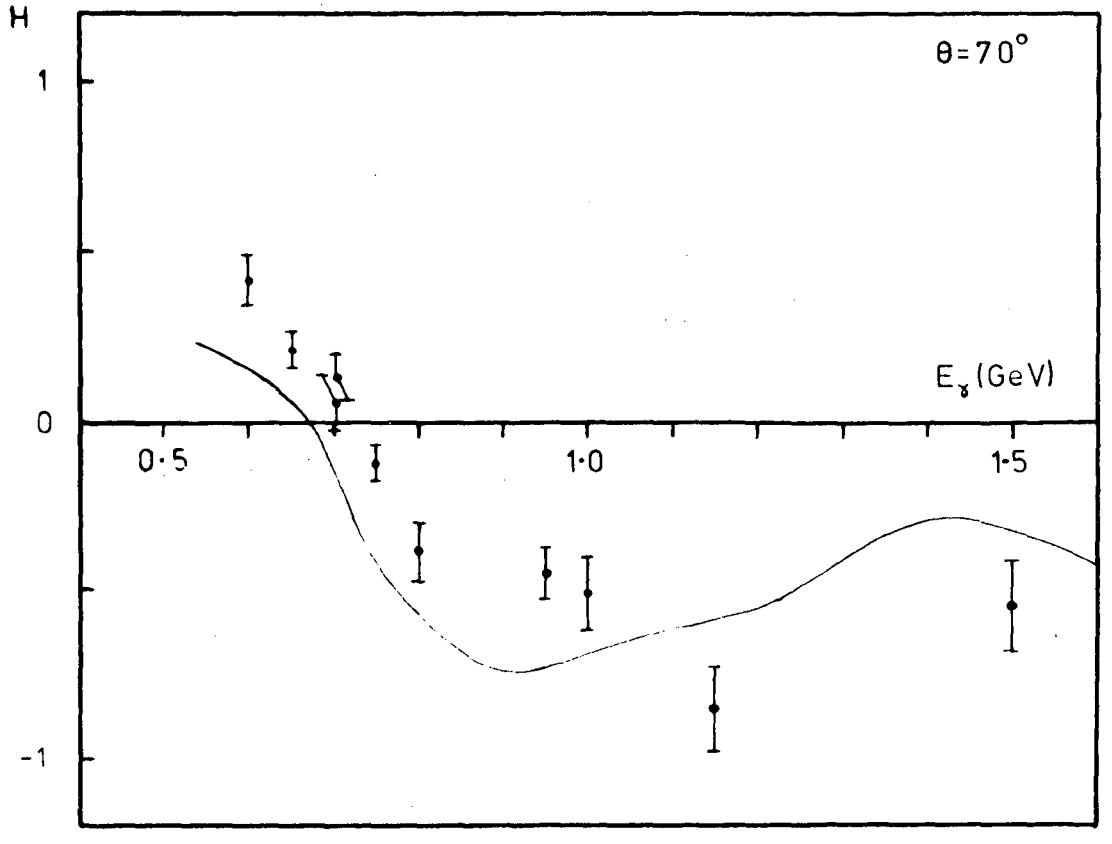

Fig. 2c

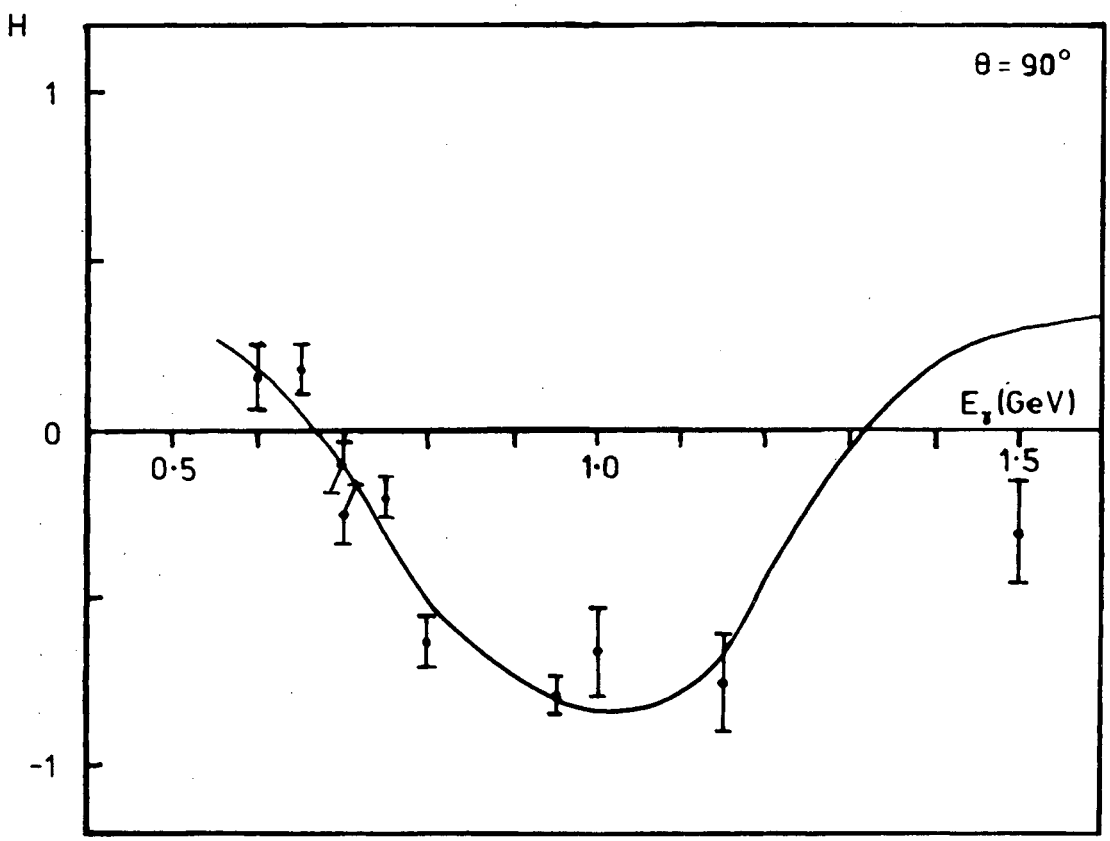

Fig. 2d

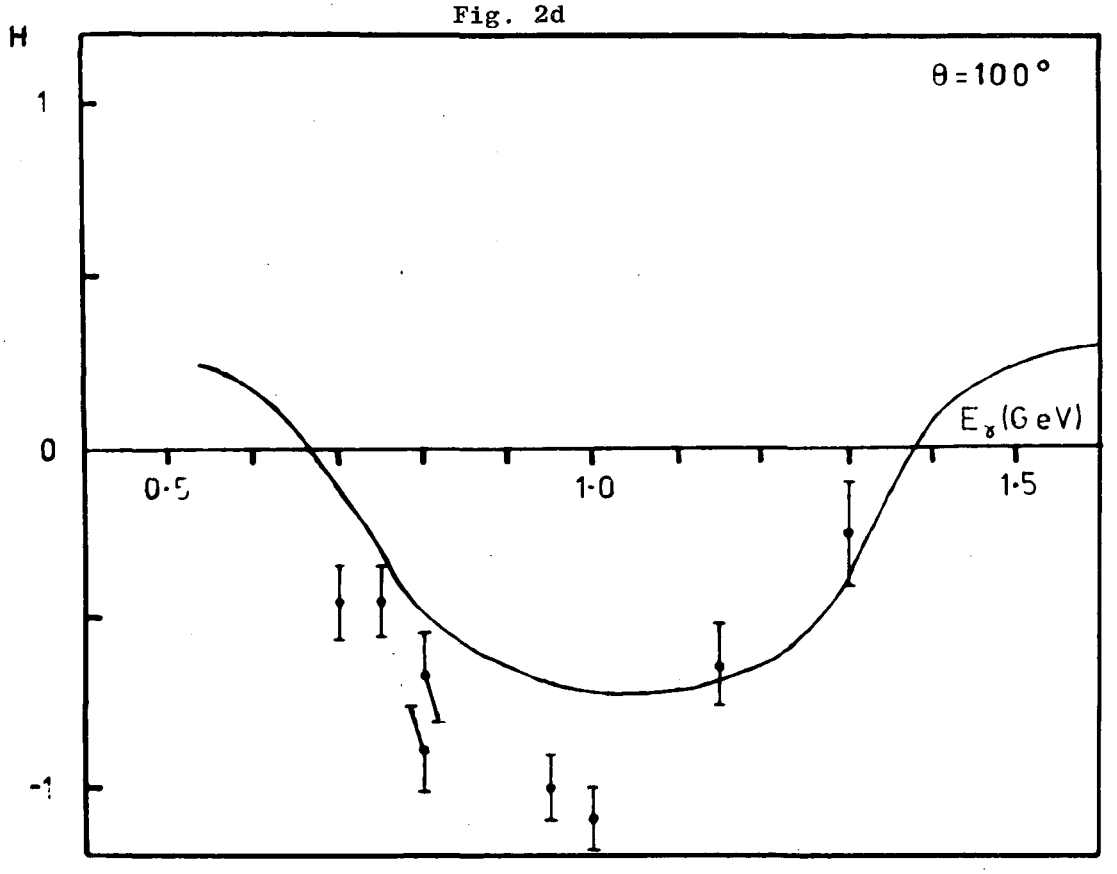

Fig. 3a

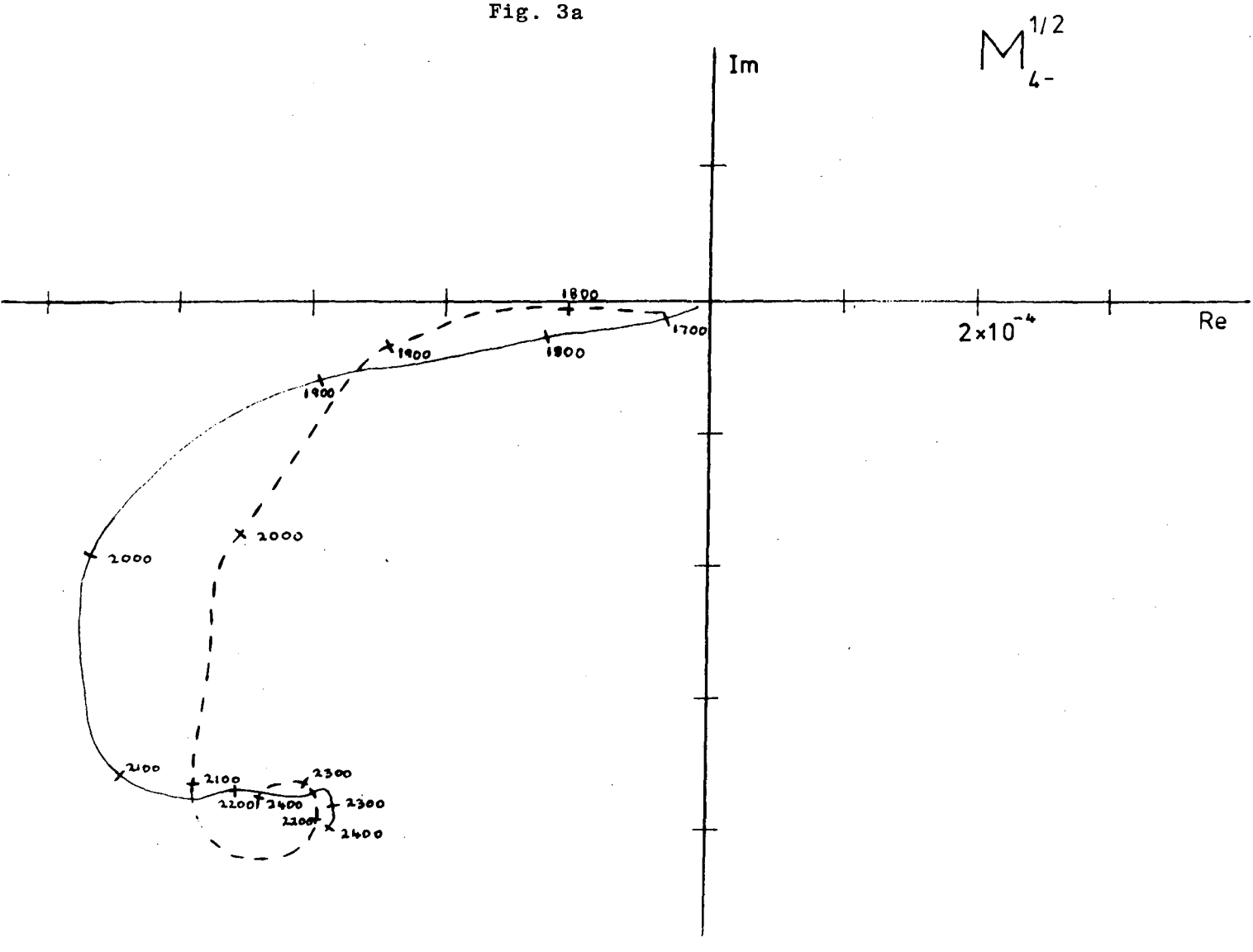
$M_{4-}^{1/2}$
Im
Re
2×10^{-4}
1800
1700
1900
1900
1900
2000
2000
2100
2100
2200
2300
2400
2200
2300
2200
2400

Fig. 3b

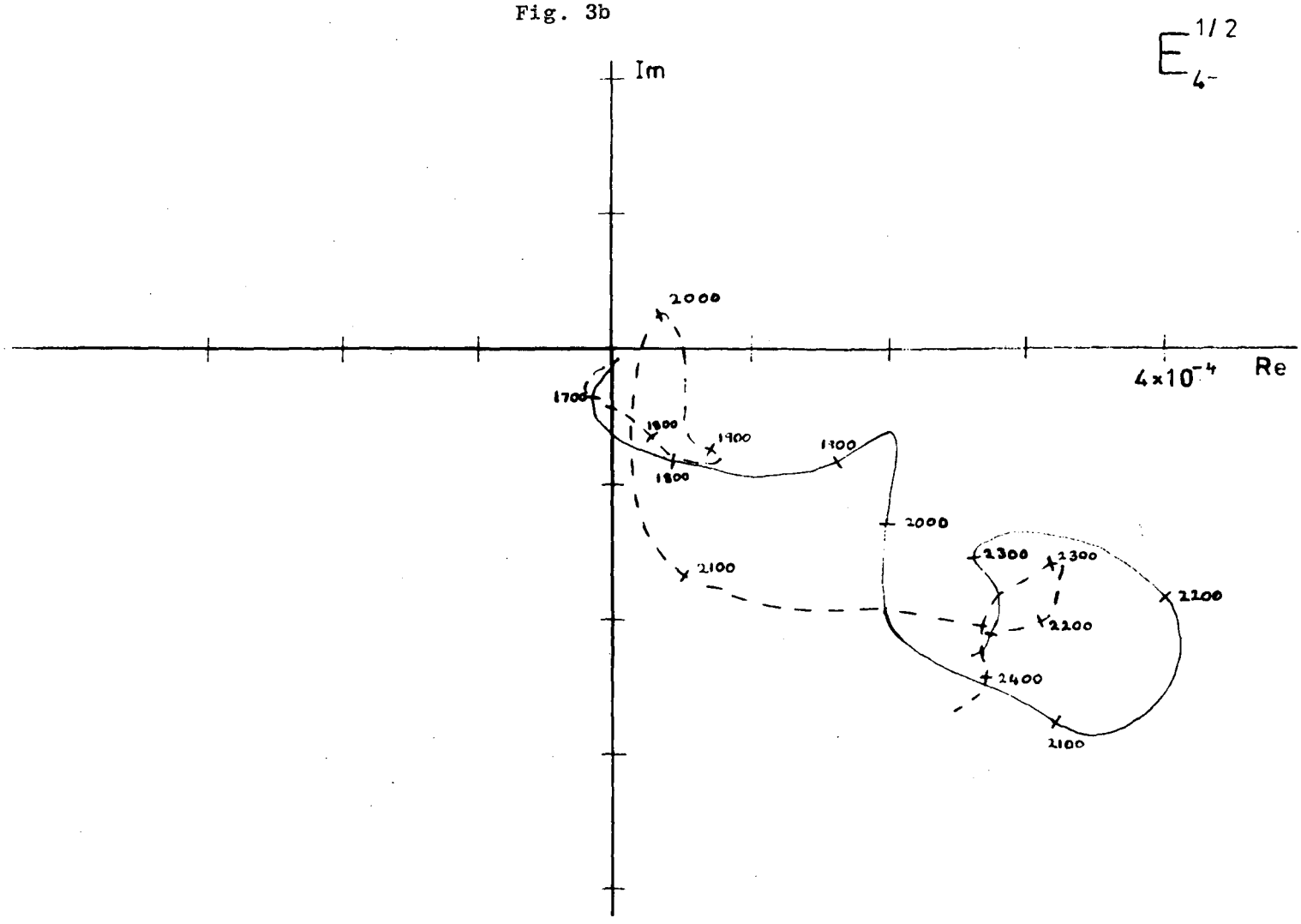
E 1/2
4-
Im
Re
4×10⁻⁴
2000
1700
1800
1900
1800
1900
2000
2100
2300
2300
2200
2200
2400
2100

Fig. 4a

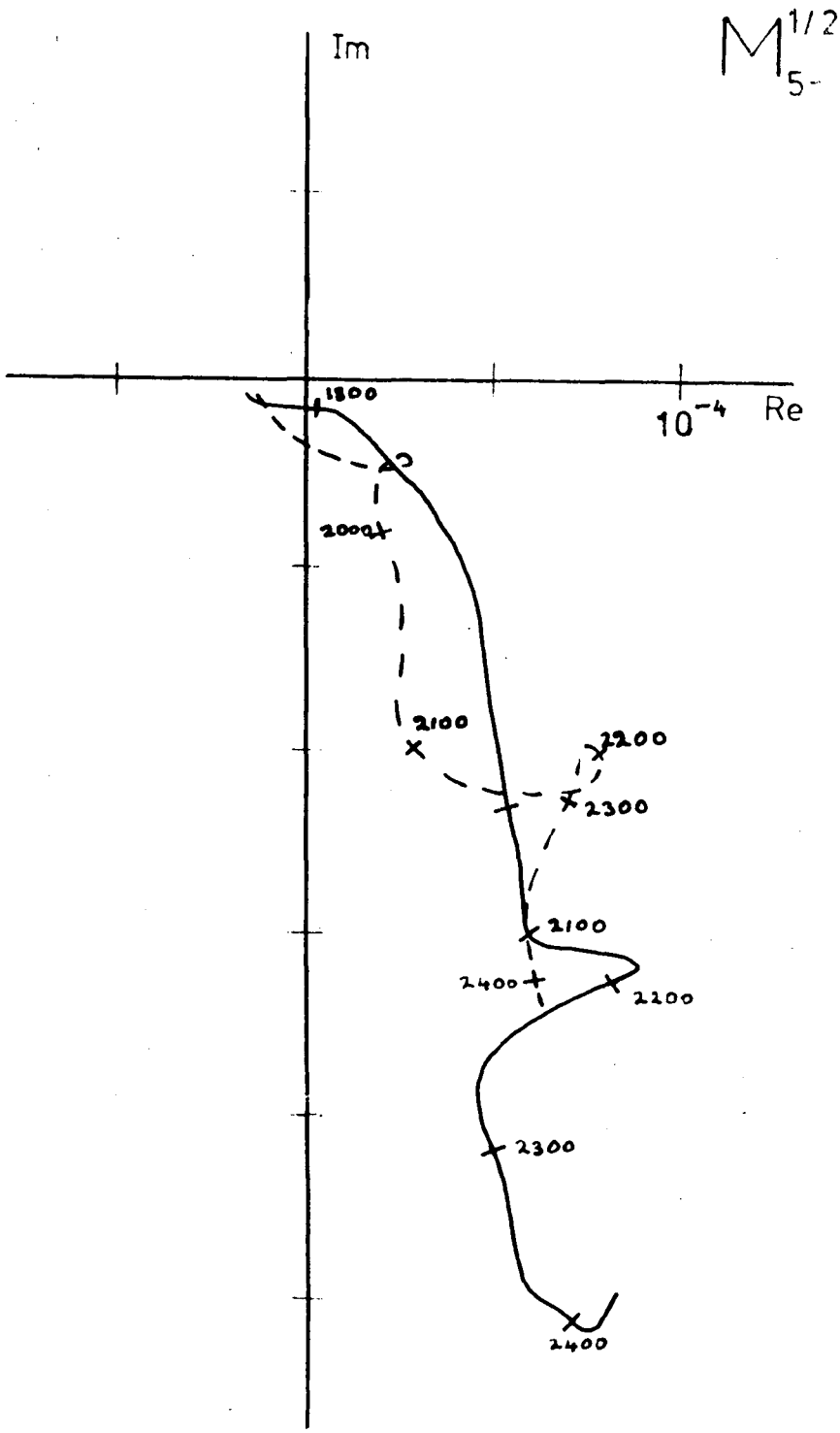
Im
$M_{5-}^{1/2}$
10^{-4} Re
1800
2000
2100
2200
2300
2100
2400
2200
2300
2400

Fig. 4b

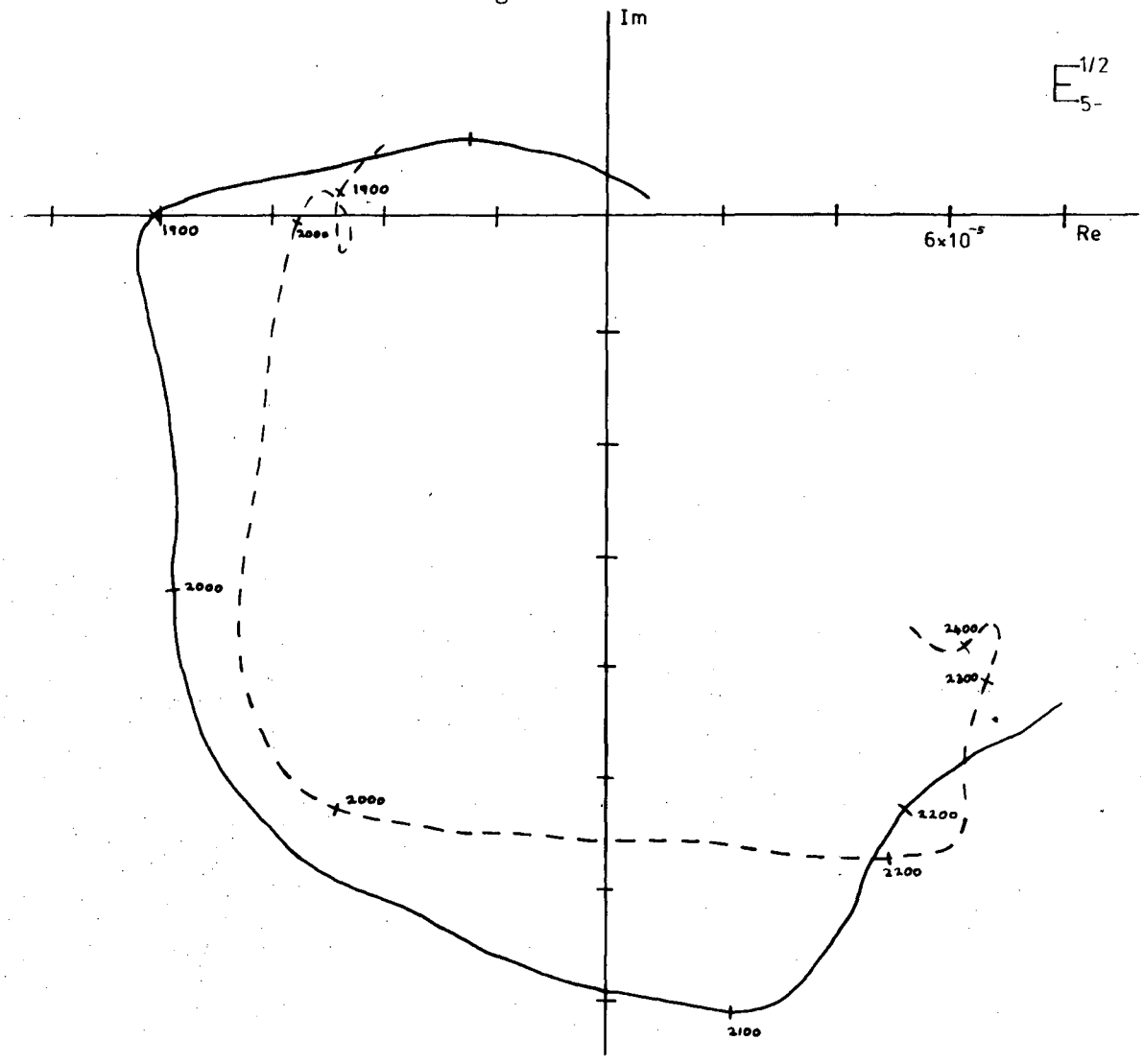
Im
$E^{1/2}$
-5-
1900
2000
1900
6×10^{-5}
Re
2000
2400
2300
2000
2100
2100
2100

Fig. 5a

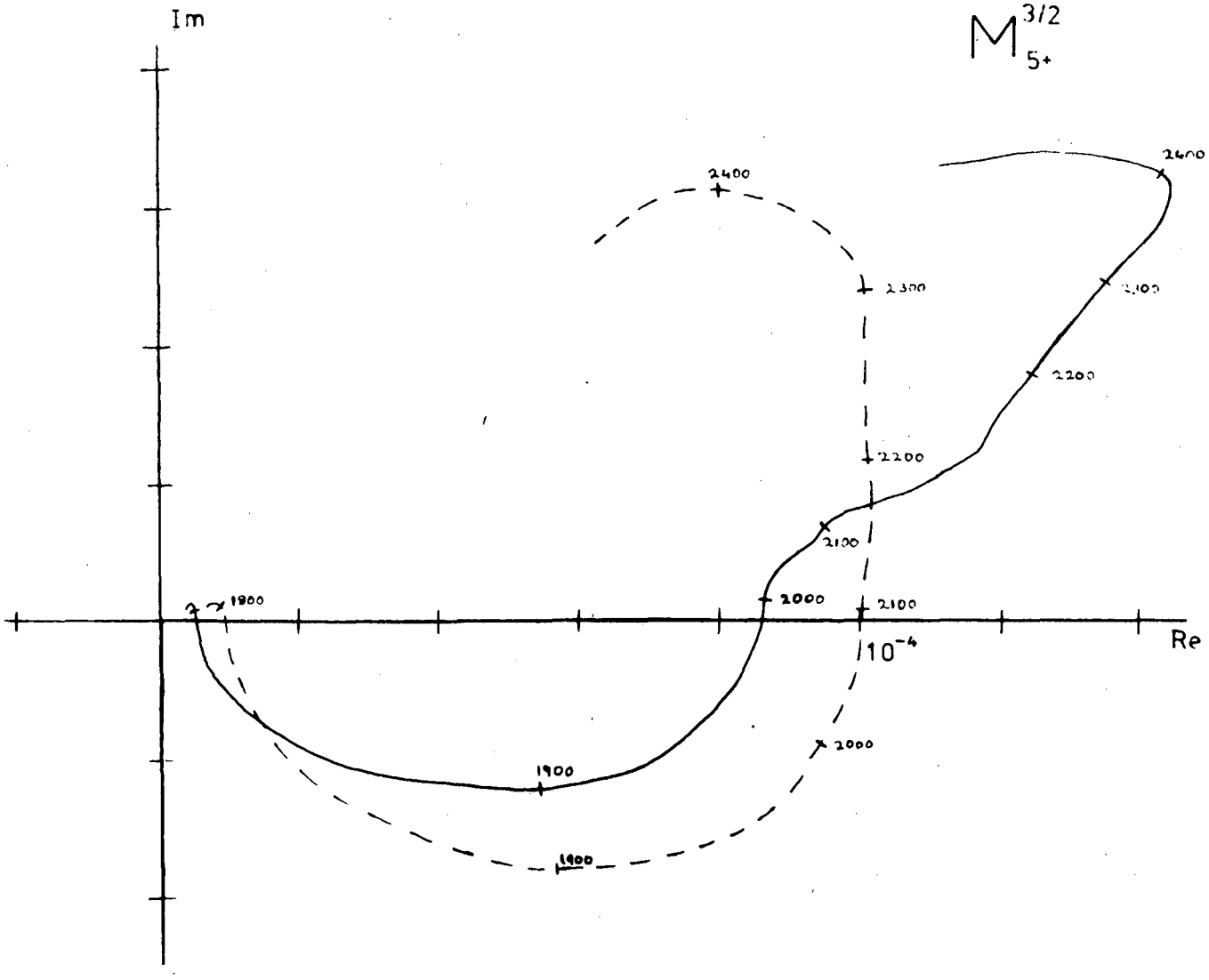
Im
$M^{3/2}_{5+}$
2400
2600
2300
2200
2200
2100
2000
2100
1900
1900
2000
1900
10^{-4}
Re

Fig. 5b

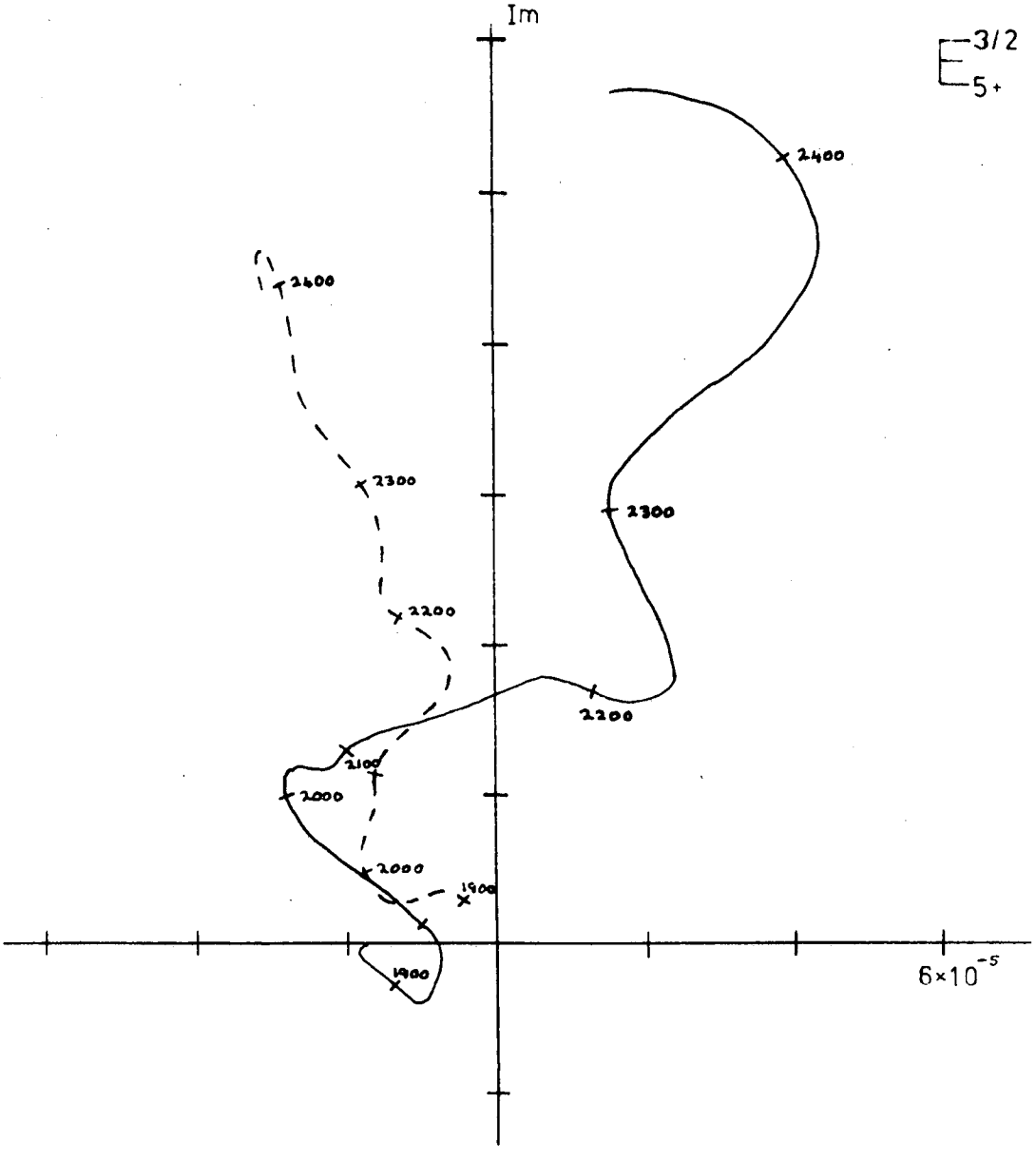
Im
E 3/2 5+
2400
2600
2300
2200
2300
2200
2100
2000
2000
1900
1900
6×10⁻⁵

This report was done with support from the Department of Energy. Any conclusions or opinions expressed in this report represent solely those of the author(s) and not necessarily those of The Regents of the University of California, the Lawrence Berkeley Laboratory or the Department of Energy.

TECHNICAL INFORMATION DEPARTMENT
LAWRENCE BERKELEY LABORATORY
UNIVERSITY OF CALIFORNIA
BERKELEY, CALIFORNIA 94720